1997051

Effect of Microstrains and Particle Size on the Fatigue Properties of Steel

by W. P. Evans and J. F. Millan

Abstract

Fatigue tests were run on notched SAE 86B45 specimens in bending at three hardness levels to determine the influence on fatigue of the X-ray measured parameters of microstrain and particle size. Changes in these quantities were produced by shot peening. The attendant macro residual stresses were shown to be equivalent to mechanically applied stresses and were compensated for by appropriate values of mean mechanical stress. Peening of the soft material produced large changes in microstrain and particle size and enhanced the fatigue limit. Peening did not alter the microstrain and particle size in the hard material.

THE EFFECT OF RESIDUAL STRESSES on fatigue strength has long been of concern to engineers interested in obtaining maximum performance from materials. A general opinion that has been held for many years is that tensile residual stresses will lower fatigue strength and the compressive residual stresses will raise fatigue strength. Fatigue tests conducted in this area in recent years have not altered this basic conclusion. However, of great practical interest is the degree of improvement, and it is to answer this question that most fatigue tests are run.

As residual stresses are conventionally defined and measured, it has seemed logical to consider them synonymous with stresses that might be produced mechanically[1]. For instance, the effect on fatigue of a tensile residual stress should be equivalent, except for gradient, to a stress of similar magnitude produced by external mechanical loading. Some recognition should also be given to the possible tendency of the actual residual stress to change or fade under the action of cyclic stressing.

In equating internal residual stresses to externally applied mechanical stresses, some anomalous effects have been observed. Bending fatigue tests on relatively soft steels have shown conclusively that the effect of mechanically simulated residual stress is small or completely absent[2]. On the other hand, true residual stresses will under certain circumstances produce effects of considerable magnitude in terms of change of fatigue strength[3].

Residual stresses are produced by heat treatment and by mechanical working. The latter may be shot peening, rolling or, less commonly, plastic extension or compression of an entire member. During the past several years, X-ray diffraction methods of measuring residual stress have been widely discussed and applied [4,5]. This method is non-destructive and permits measurement of the high stress gradients that may occur close to a surface, which are highly useful characteristics for correlation with fatigue tests. The important possibility, with regard to the present paper, is that the X-ray method can measure other variables arising from the heat treating or mechanical working process. Specifically, the variables to be defined and discussed will be called microstrain and particle size.

Both hardening and cold working affect the residually strained state, which includes macrostress, microstrain, and particle size. Usually, the three X-ray parameters change together and it is difficult to determine their individual contributions to strength.

The purpose of the present work is to determine the residually strained state by X-ray diffraction and to attempt to correlate both macro and micro concepts of strain and particle size with fatigue results. The work covers X-ray and bending fatigue tests on SAE 86B45 steel specimens, quenched and tempered to various hardnesses. Some of the specimens of each hardness level were cold worked by shot peening. Residual stress due to peening could be cancelled or nearly cancelled by a mean mechanical stress superimposed on the alternating component during cycling. In this way, the combined effects of microstrain and particle size could be independently studied.

The X-ray results are compared with similar information on SAE 1045 steel previously reported[6]. Some data on SAE 8645 steel is also included for comparison.

Definitions

Microstrain can be defined in terms of its "macro" counterpart. As adopted recently by SAE ISTC, Div. 4[7]:

"Macrostress is the mean stress over the gage length of measurement..."

"Microstrains are the strains being averaged by the macro measurement..."

Though the size of the given gage length doesn't matter, it is usually presumed that microstrains exist over regions too small to measure.

A mechanical analogy to this situation is described by a hypothetical strain gage whose gage area is imagined to be covered by many components (Fig. 1). The gage as a whole measures an average or mean strain, while any component would indicate a microstrain. Variable microstrains produce rms strain deviations from the mean strain, which are determined by X-ray line broadening analysis.

The spacing of the atomic planes within a crystal or grain may also be used as a measure of strain. X-rays are diffracted from atomic planes of proper orientation. The angle of diffraction or peak position can be measured and is related to atomic spacing and hence, strain. Strain determined in this way is an average strain in a direction normal to the crystallographic planes contributing to the diffraction. Because it is an average, it is a macrostrain.

But as was true in the strain gage analogy, the X-ray peak in reality is a blending together of many unresolved peaks (Fig. 2).

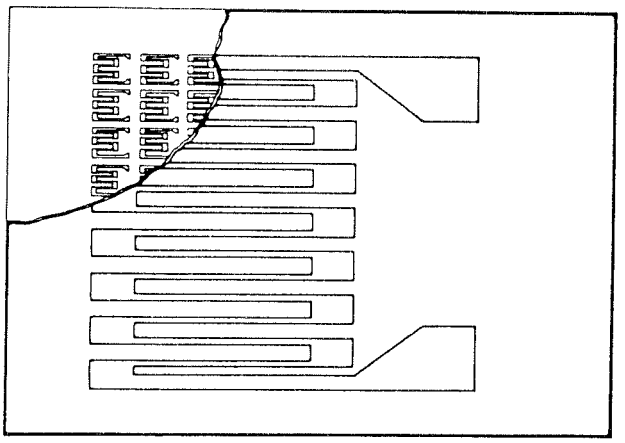

Fig. 1. Strain gage showing hypothetical components

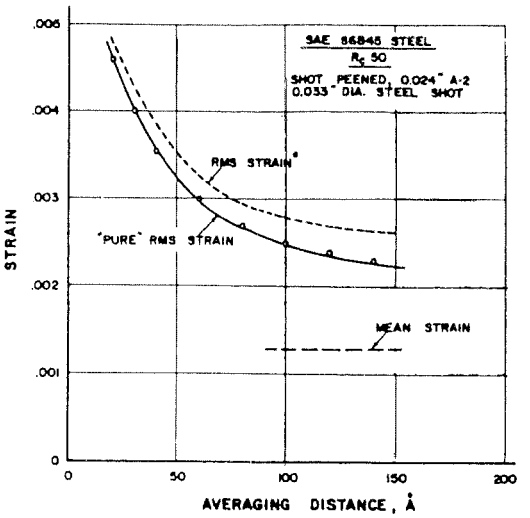

Fig. 3. Typical X-ray strain data. RMS strain is calculated from "pure" RMS strain showing effect of mean strain*

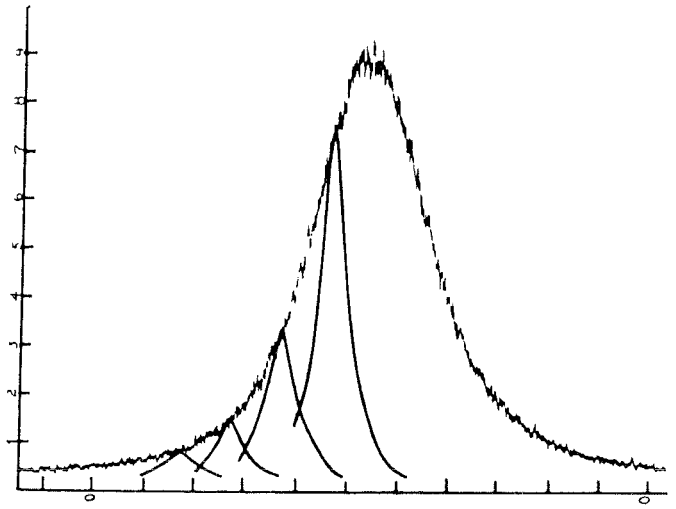

Fig. 2. X-ray peak showing hypothetical components

Each sub-peak represents diffraction of X-rays from separate micro regions. If the strain is non-uniform from one region to the next, then the X-ray peak will be broadened because of the variable position of the micro peaks.

Small particle or sub-grain size also causes X-ray line broadening and Warren and Averbach[8,9] have shown through Fourier analysis of X-ray line shapes how both kinds of broadening can be separated in terms of their respective Fourier coefficients. A particle is defined as a small region within a crystal or grain which diffracts X-rays coherently. It is of given orientation and may be bounded by small angle grain boundaries, twin boundaries, dislocations, or stacking faults. Particle size is calculated as a distance in A° and microstrain is calculated as rms strain averaged over particular column or gage lengths.

Typical strain data is shown in Fig. 3 as a function of averaging distance within the crystal. The averaging distance is the column length, L, calculated from the range used in the harmonic analysis. A crystal or grain is visualized as columns of cells over which rms strains are averaged. Rms strains may vary over micro regions but approach the mean value as the averaging distance increases. Usually, rms strain values are read off such plots at an average distance of 30 - 50A°.

Table 1
Chemical Analyses of Steels
Weight Percent

Element	SAE 86B45	SAE 8645
C	0.45	0.43
Mn	0.80	0.85
S		0.005
P		0.011
Si	0.33	0.30
Ni	0.47	0.54
Cr	0.54	0.56
Mo	0.20	0.23
Cu	0.18	0.08
Al		<0.03
Sn		
B	0.0014	Nil

Methods

Specimen Preparation - X-ray and fatigue tests were run on SAE 86B45 steel of chemical composition shown in Table 1. Three hardness levels were used and some specimens of each hardness were shot peened. Bar stock of 3-3/8 in. diameter was normalized at 1600 F in a neutral atmosphere for 2-1/2 hr. Specimens were then rough machined and austenitized at 1500 F for 2-1/2 hr in a neutral atmosphere, oil quenched, and tempered at 550 F for 2 hr in air. They were then finished machined as shown in Fig. 4 and retempered in argon for 2-1/2 hr. Hardness levels of Rockwell C 20, 35, and 50 were produced by tempering temperatures of 1280, 1080, and 670 F, respectively. Approximately 0.0025 in. was removed from the notch surface by electropolishing to remove a slight stain produced by tempering. Some of the specimens of each hardness group were then peened to an Almen intensity of 0.024 in. A-2 using 0.033 in. diameter steel shot. X-ray measurements were made on the notch surface. The reference for the X-ray line broadening work was electrolytic iron powder, passed through No. 325 mesh screen. A thin layer of powder was coated on a synthane specimen of similar notch geometry, thinly greased with petroleum jelly.

Some X-ray analyses were carried out on SAE 8645 steel for comparison. Specimens of 1-3/4 in. diameter were machined from steel bar stock of composition shown in Table 1 and austenitized at 1520 F in a neutral atmosphere, oil quenched, and

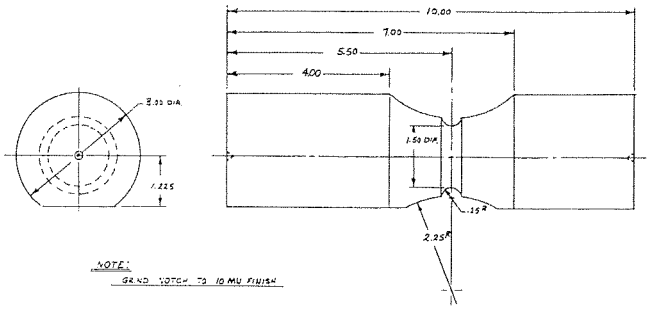

Figure 4. Fatigue specimen

tempered. Surface hardness levels of Rockwell C45 and 54 were produced by tempering temperatures of 800 and 300 F, respectively. X-ray analyses were carried out on electropolished cross-sections near the curved edge of the bars. The X-ray reference for this work was an annealed and stress relieved bar of SAE 8645 steel of similar geometry. The bar was heated in argon at 1650 F for 1 hour and slow-cooled.

Fatigue Tests - The fatigue machine used in these tests was designed specifically for this investigation. It was a non-rotating, bending machine with provision for applying mean loads other than zero. By utilizing the principle of inertia force compensation, the stress at the critical section of the specimen was directly proportional to the centrifugal force of the rotating exciter weight. The machine then becomes an essentially constant load type of machine, as contrasted to a constant deflection type. It operated at a speed of 1800 rpm with an alternating stress capacity of this specimen of ±200,000 psi. Mean stresses could be applied to 200,000 psi. A microswitch was positioned to shut down the machine upon failure of the specimen. An electric clock recorded time to failure. Cycles to failure were determined by multiplying this time by the exciter motor rpm.

The machine was calibrated by the use of a strain gage in the notched portion of a specimen. A C6 1X32 strain gage was used for this purpose. The stress figures that will be quoted are, therefore, the surface maximum principal stresses in the notch in a direction parallel to the longitudinal axis of the specimen. The theoretical stress concentration factor was 1.5 as determined by charts derived by Lipson[10].

The construction of the fatigue machine that permitted the application of an initial mechanical stress in bending, placed the upper side of the notched portion of the specimen in controlled tension. This stress also was parallel to the specimen axis. The net mean stress was considered to be the algebraic sum at the surface of the mean mechanical stress and the measured residual stress. By this means, it was possible to produce a net mean stress of substantially zero in a peened specimen in which the residual stress at the surface was compressive. No attempt was made to balance mechanical and residual stresses in the tangential direction or in depth.

Measurements of residual stresses on specimens that had been cycled at the fatigue limit indicated inconsequential changes of stress. This justified the concept of balancing the residual stress with a constant mechanical stress throughout the life of the specimens. An average of seven specimens were run for each of 12 curves to establish the fatigue limit.

X-Ray Technique - Microstrains were determined as rms strain deviations from the mean. The Warren and Averback[8,9] line broadening analysis was used as reviewed by Warren[11] and applied to studies of the substructure of steels by Evans and Buenneke[6].

On the SAE 86B45 specimens, the X-ray measurements were made in the notch on the side of subsequent fracture on representative specimens prior to fatigue testing. A G.E. XRD-5 diffractometer and proportional counter detector was used. Peak profiles were point-counted for greater accuracy in the broadened peaks. Maximum increments of 0.5 deg 2θ were used in the tail regions and 0.01-0.05 deg 2θ increments in the peak regions. Usually, chromium Kα radiation was used for the 110 peaks and cobalt Kα radiation for the 220 peaks. A minimum of 10,000 counts per point was used in the tail regions and 40,000 counts per point in the peak regions. Net intensities were corrected by L-P factors, $(1 + \cos^2 2\theta/\sin^2 \theta$, prior to the harmonic analysis. The angular 2θ positions were converted to units of $\sin\theta/\lambda$ at increments of 0.00005, calculated by parabolic interpolation between measured points. The harmonic analysis was carried out on a Control Data G-20 digital computer over a total range of 0.10 for all peaks, and centered on the midpoint of the respective peak in all cases.

Rms strains determined from such data were called "pure" rms strains, since the effect of the mean strain on the rms results had been removed. Peak profiles from the reference were chart recorded at a speed of 60 in./hr. Scanning speed of the goniometer was 0.2 deg 2θ per minute, using an 8 sec time constant. A beam slit of 1 deg horizontal divergence and reduced vertical size was used with a 0.2 deg detector slit giving a beam size at the specimen of approximately 0.06 in. horizontally and 0.20 in. vertically. Specimens were oriented on the goniometer so that the cylindrical axis was vertical. Rms strain and particle size were calculated in the <110> crystallographic direction, normal to the notch surface and the diffracting planes.

Surface macro residual stresses were calculated in the longitudinal direction from measurements in the notch by methods discussed elsewhere[4]. For this work the specimens were oriented on the goniometer so that the cylindrical axis was horizontal. The 211 peak was used, using angles of incidence of $\psi = 0$ deg and $\psi = 30$ deg.

On the SAE 8645 specimens, all line broadening data was chart recorded as above on electropolished sections. Because of the somewhat narrower peak, a range of 0.05 units of $\sin\theta/\lambda$ was used in the harmonic analysis.

Some rms strain data on SAE 1045 steel, previously reported[6], was recalculated as "pure" rms strain, $\langle\varepsilon^2\rangle^{1/2}$ pure, by removing the effect of the mean strain, $\langle\varepsilon\rangle$. If the strain distribution is Gaussian[12], then this may be done by the relation

$$\langle\varepsilon^2\rangle^* = \langle\varepsilon^2\rangle \text{ pure} + \langle\varepsilon^2\rangle \qquad (1)$$

where $\langle\varepsilon^2\rangle^*$ is the mean square strain obtained with the effect of the peak shift left in the harmonic analysis.When the center of the range used in the harmonic analysis is taken as the respective peak center, then mean strain effect is automatically eliminated. Pure rms strains are then obtained directly from the Fourier coefficients and Eq. 1 is not necessary.

Results

X-Ray - The effect of hardening on rms strain and particle size is shown in Figures 5 and 6 for three steels. The rms strains for these and similar plots are averaged over gage or

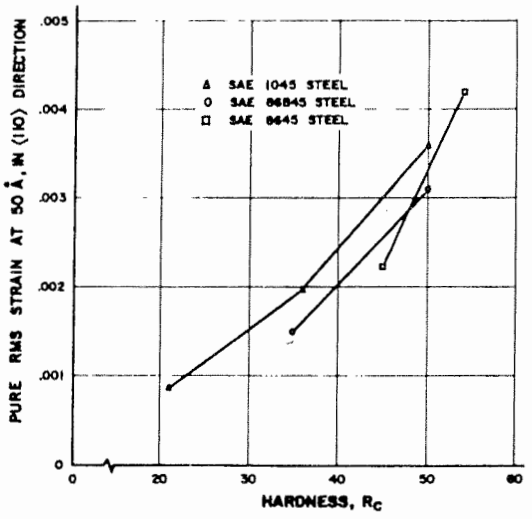

Figure 5. Effect of hardening on RMS strain

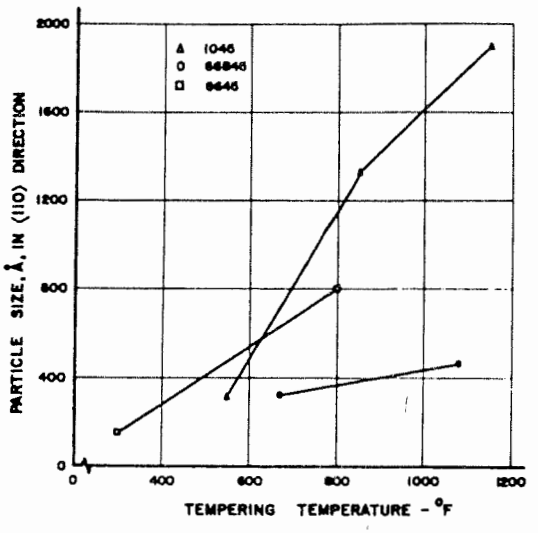

Figure 8. Effect of tempering on particle size

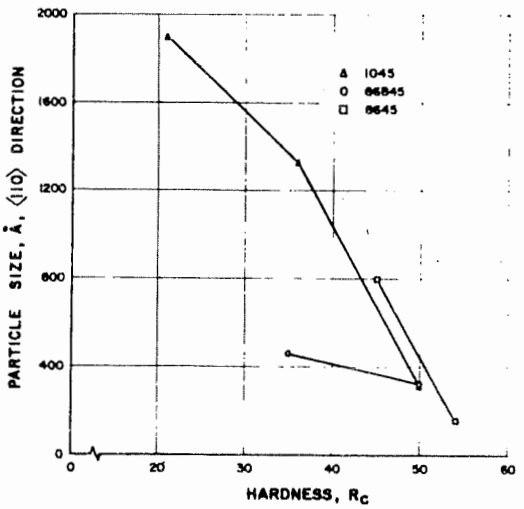

Figure 6. Effect of hardening on particle size

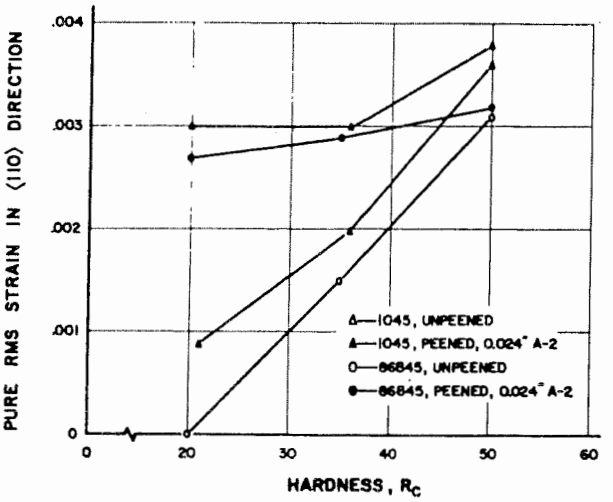

Figure 9. Effect of peening on RMS strain as function of hardness

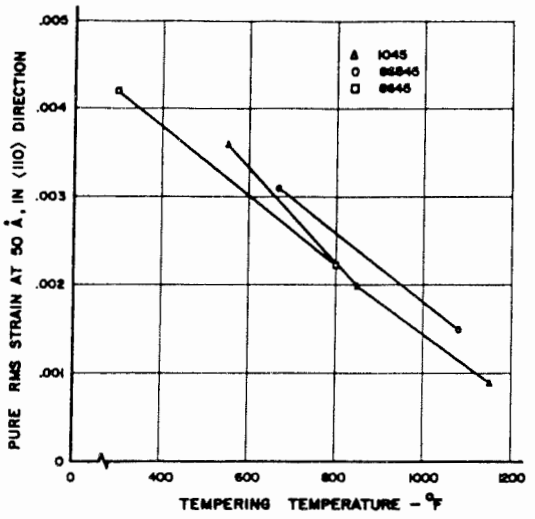

Figure 7. Effect of tempering on RMS strain

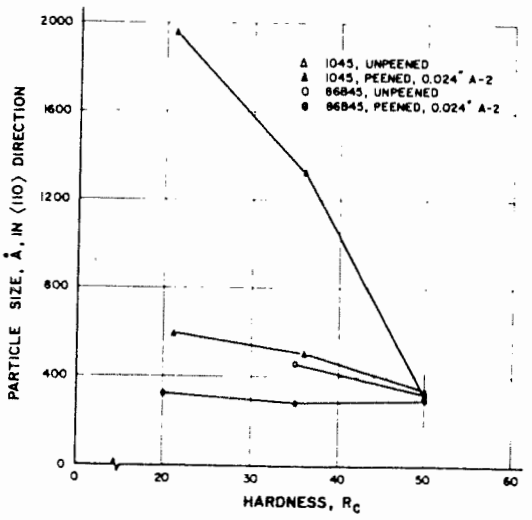

Figure 10. Effect of peening on particle size as function of hardness

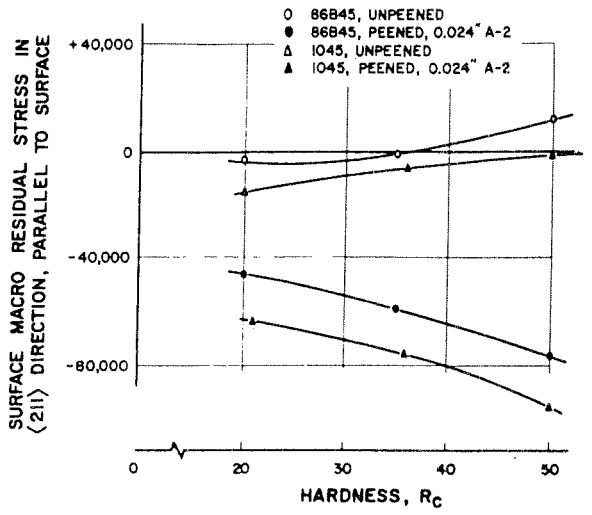

Figure 11. Effect of peening on macro residual stress in psi as function of hardness

Table 2 - Average Surface Residual Stresses of the Fatigue Specimens, SAE 86B45 Steel

Macro Residual Stress in Notch in Longitudinal Direction, psi

Hardness	Unpeened	Peened
Rc 50	+12,000[14]*	-76,000[11]
Rc 35	-800[6]	-59,000[8]
Rc 20	-3,000[2]	-45,000[7]

*Refers to number of separate specimens measured.

column lengths of 50 A°. In general, rms strain increased with hardness and particle size decreased. The boron steel had a smaller particle size at low hardness. The effect of the temperature of tempering, Figures 7 and 8, was similar. Rms strain decreased and particle size increased as the temperature was increased. Again the boron steel showed a markedly smaller particle size and this may be one of the significant effects of boron. Cold working by shot peening increased the rms strain and decreased the particle size, Figures 9 and 10. Peening had less effect as the hardness increased, and at Rc 50 no significant changes was produced by peening. This agreed with previous work[6].

Figure 11 shows the effect of peening on surface macro residual stress. Peening induced a high level of compressive stress which increased as the hardness increased, unlike rms strain and particle size. Numerical values of residual stress in the notch for peened and unpeening specimens at the three hardness levels run in fatigue are listed in Table 2. As is seen, the residual stresses before peening were low.

Correlation with Fatigue Tests - Fatigue test results are shown in Figures 12 - 14 for the Rc 50, Rc 35, and Rc 20 specimens, respectively. The fatigue limit information from these three curves is summarized on the graph in Figure 15 in which the alternating stress at the fatigue limit is plotted against the net mean stress at the surface of the critical section. This figure is plotted for four conditions for each of the three hardnesses, as follows:

1. Peened with no mechanical mean stress.
2. Peening with sufficient mechanical mean stress to bring the surface stress to zero, or close to zero.

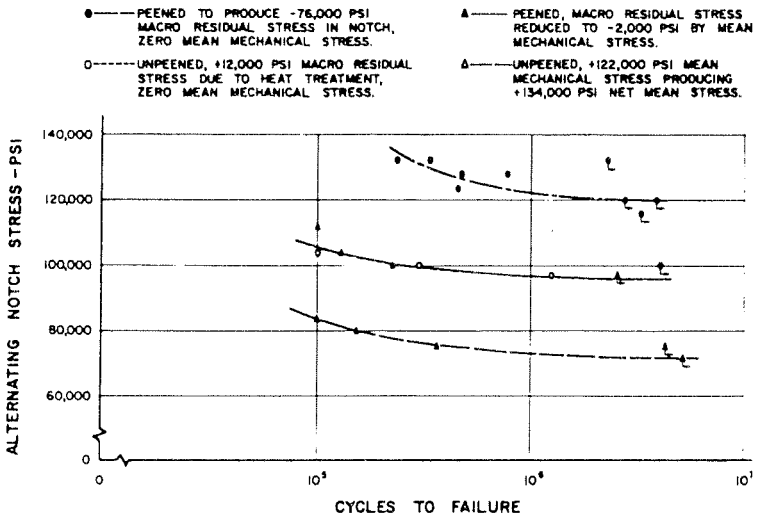

Figure 12. S-N Curves, SAE 86B45 Steel, Rc 50

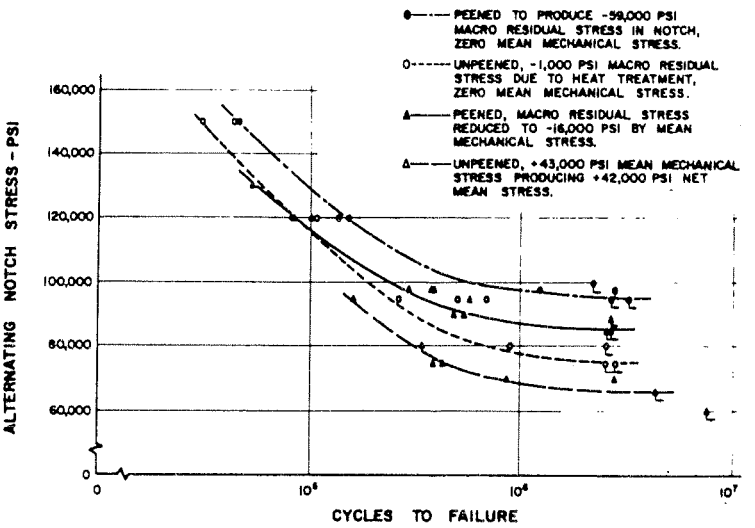

Figure 13. S-N Curves, SAE 86B45 Steel, Rc 35

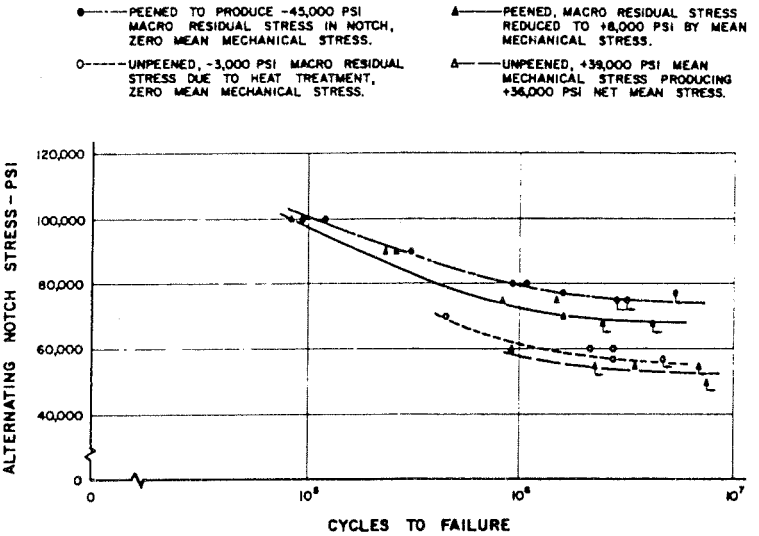

Figure 14. S-N Curves, SAE 86B45 Steel, Rc 20

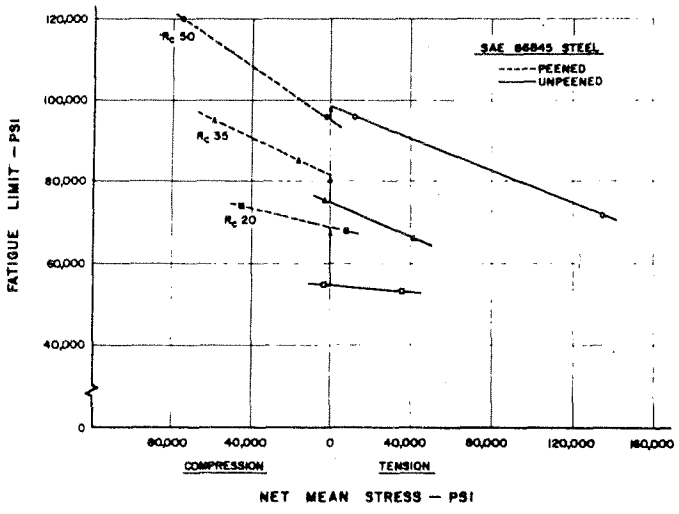

Figure 15. Effect of peening on fatigue limit as function of hardness

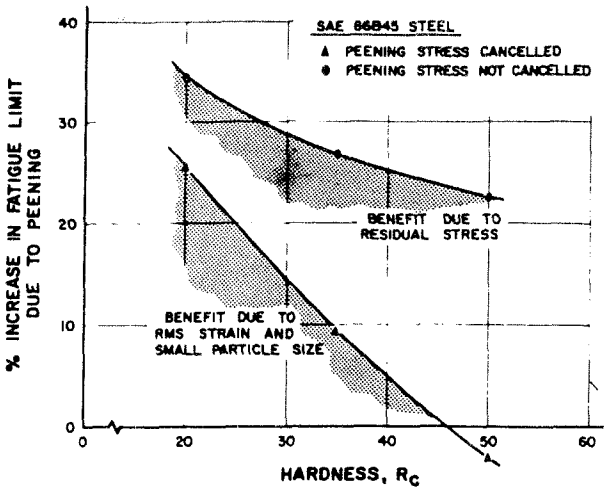

Figure 16. Per cent increase in fatigue limit due to peening as function of hardness

3. Unpeened with no mechanical mean stress and with a residual stress of zero or nearly so.
4. Unpeened with a mechanical mean tensile stress.

Attention is called to the principal features of these plots which is the indicated difference in fatigue limits at a net mean surface stress of zero. This difference may be noted as 69,000 - 55,000 or 14,000 psi for the Rc 20 specimens; 82,000 - 75,000 or 7000 psi for the Rc 35 specimens; and 95,000 - 98,000 or -3000 psi for the Rc 50 specimens.

The slopes of these plots indicated comparative sensitivity to the effect of mean stress. The maximum slope exists at Rc 50 and the minimum at Rc 20. The slopes of the portions of the curves representing the peened condition are somewhat steeper than those portions representing the unpeened conditions.

DISCUSSION

In general, both hardening and cold working by peening tend to increase rms strain and decrease particle size. The steel with boron showed a markedly lower particle size at all conditions. Rms strains decreased and particle size increased as the temperature of tempering increased. Evidently, rms strains are relieved by tempering, and this should provide a means of altering the magnitude of rms strain produced by cold working.

It is thought significant that the line broadening parameters, that is, rms strain and particle size, were essentially unchanged by peening at a hardness of Rc 50. Previous work[6] on SAE 1045 steel showed this trend at this hardness level even at much higher peening intensities. Evidently, at Rc 50 the material is "saturated" with the short-range microstrains produced by hardening alone. This seems to agree with strain hardening data obtained by Polakowski[13] and others. At a hardness range of Rc 40 - 50, the strain hardening exponent, n, is low and little strain hardening by working is expected. Below or above this hardness range, n increases again. This means that above Rc 50, the material should absorb additional strain hardening with accompanying changes in rms strain.

Peening did affect macro residual stress, however, at all hardnesses. The induced stresses by peening were compressive and increased in magnitude with initial hardness. Macro stresses are of longer range and must be balanced throughout the entire body. If specimens are small enough to "through-harden," then transformation stresses are essentially cancelled and little residual stress will result if thermal stresses are low. Such was the case for both steels reported, and peening, being a surface effect, greatly altered the surface residual stress condition.

Peening improved fatigue strength at all hardnesses (Figures 12 - 14), but for different reasons. At Rc 50 (Figure 12) the improvement was mainly due to the high magnitudes of induced compressive macro residual stress. When the peening stresses were cancelled by mean mechanical load, the fatigue strength was nearly equivalent to that of the unpeened bars. This showed the equivalence of mechanical stress and macro residual stress in bending fatigue.

At Rc 50, unpeened and peened data formed nearly continuous curves through zero net mean stress (Figure 15). This is expected because at this hardness, rms strain and particle size were essentially unchanged by peening (Figures 9 and 10). As the hardness decreased, macro residual stress had less effect. This is shown by the decreasing slopes of Figure 15. But another effect is noted, namely, the displacement or "step" between peened and unpeened data at zero net mean stress, which was more pronounce as hardness decreased.

Fatigue limit - line broadening data is tabulated in Table 3 and shows increasing change in rms strain and particle size due

Table 3 - Fatigue Limit Related to RMS Strain and Particle

	RMS Strain at 50A°			Particle Size, A°			Fatigue Limit at Zero Net Mean Stress		
Hardness RC	Unpeened	Peened	% Inc.	Unpeened	Peened	% Dec.	Unpeened	Peened	% Inc.
50	0.0031	0.0032	3.23	325	300	7.7	98	95	-3.06
35	0.0015	0.0092	93.3	465	290	37.6	75	82	9.35
20	≈0	0.0027	>100	Large	330	≈100	55	69	25.5

to peening as hardness decreased. This was in direct correspondence to the increasing fatigue limit due to peening as the hardness decreased, and seems to indicate a relation between the line broadening parameters and fatigue limit.

Figure 16 shows the separate effects of macro residual stress and line broadening as a function of hardness. The upper curve represents the per cent increase in fatigue limit due to peening as compared to unpeened data, the latter at zero net mean stress. The lower curve shows the per cent increase at zero net mean stress for both. At zero net mean stress the surface macro residual stresses for both peened and unpeened specimens are cancelled by definition; therefore, the increase in fatigue limit at Rc 35 and Rc 20 must be related to the increased microstrain and smaller particle size produced by peening. By difference, the benefit due to macro residual stress alone is shown.

SUMMARY

Rms strain increased and particle size decreased with hardening or cold working by peening. At Rc 50 the material was apparently "saturated" with the short-range rms strains due to hardening alone, and working by peening produced little further change. This may be related to the strain hardening exponent which indicates little strain hardening expected at this hardness level. The long-range macro residual stresses increased in compression due to peening as the hardness increased, in contrast to the microstrains.

Fatigue strength increased with peening at all hardnesses, but for different reasons. At Rc 50 the increase was due mainly to the high level of induced compressive macro residual stress. Peened and unpeened specimens had similar fatigue limits for a given net mean stress. This was explained by the fact that peening did not change microstrain and particle size at this hardness level. This also showed the equivalence of mean mechanical stress and macro residual stress in bending fatigue.

Peening of the soft material produced large changes in rms strain and particle size and enhanced the fatigue limit. The displacement (or step) in the fatigue limit - net mean stress plot was related to these changes.

REFERENCES

1. JoDean Morrow and J.F. Millan, "Influence of Residual Stress on Fatigue of Steel," SAE TR-198, (1961), 4, 5.
2. H.J. Gough, "Some Experiments on the Resistance of Metals to Fatigue Under Combined Stresses," Aeronautical Research Council, R. and M. 2522, His Majesty' Stationery Office, (1951), 124.
3. Charles Lipson and Robert C. Juvinall, "Handbook of Stress and Strength." The Macmillan Co., (1963), 141.
4. A.L. Christenson, et al., "The Measurement of Stress by X-Ray," SAE TR-182, 1960.
5. D.E. Martin, "Evaluation of Methods of Measurement of Residual Stress," SAE TR-147, 1960.
6. W.P. Evans and R.W. Buenneke, "X-Ray Line Broadening of Hardened and Cold Worked Steel," Trans. Met. Soc. AIME, Vol. 227, (April 1963), 447-451.
7. W.P. Evans and W.E. Littmann, "Macro and Micro Residual Stresses," SAE Journal, Vol. 71, (March 1963), 118 - 121.
8. B.E. Warren and B.L. Averbach, "The Effect of Cold Work Distortion on X-Ray Pattern," J. Appl. Phys., Vol. 21, (1950), 595-599.
9. B.E. Warren and B.L. Averbach, "The Separation of Cold-Work Distortion and Particle Size Broadening in X-Ray Patterns," J. Appl. Phys., Vol. 23, (1952), 497.
10. Charles Lipson and Robert C. Juvinall, "Application of Stress Analysis to Design Metallurgy," University of Michigan, (1961), 232.
11. B.E. Warren, "X-Ray Studies of Deformed Metals," Progress in Metal Physics, New York: Pergamon Press, Vol. 8 (1959), 147 - 202.
12. J.B. Cohen and W.P. Evans, to be published.
13. N.H. Polakowski, "Observations on the Mechanical Behavior of Heat-Treated Steels at High Hardness Levels," J. Iron and Steel Inst., Vol. 185, (1957), 67.